Loughborough University

This item was submitted to Loughborough's Research Repository by the author.
Items in Figshare are protected by copyright, with all rights reserved, unless otherwise indicated.

Agitation and aeration of stirred-bioreactors for the microcarrier culture of human mesenchymal stem cells and potential implications for large-scale bioprocess development

PLEASE CITE THE PUBLISHED VERSION

https://doi.org/10.1016/j.bej.2018.04.011

PUBLISHER

© Elsevier

VERSION

AM (Accepted Manuscript)

PUBLISHER STATEMENT

This work is made available according to the conditions of the Creative Commons Attribution-NonCommercial-NoDerivatives 4.0 International (CC BY-NC-ND 4.0) licence. Full details of this licence are available at: https://creativecommons.org/licenses/by-nc-nd/4.0/

LICENCE

CC BY-NC-ND 4.0

REPOSITORY RECORD

Heathman, Thomas R.J., Alvin W. Nienow, Qasim A. Rafiq, Karen Coopman, Bo Kara, and Christopher J. Hewitt. 2018. “Agitation and Aeration of Stirred-bioreactors for the Microcarrier Culture of Human Mesenchymal Stem Cells and Potential Implications for Large-scale Bioprocess Development”. figshare. https://hdl.handle.net/2134/33392.

Agitation and aeration of stirred-bioreactors for the microcarrier culture of human mesenchymal stem cells and potential implications for large-scale bioprocess development

Thomas R.J. Heathman

Hitachi Chemical Advanced Therapeutics Solutions, LLC, 4 Pearl Ct, Allendale, New Jersey 07401, USA

Centre for Biological Engineering, Loughborough University, Leicestershire, LE11 3TU, UK

Alvin W. Nienow

Aston Medical Research Institute, School of Life and Health Sciences, Aston University, Aston Triangle, Birmingham, B4 7ET

Centre for Biological Engineering, Loughborough University, Leicestershire, LE11 3TU, UK

Centre for Bioprocess Engineering, University of Birmingham, B15 2TT, UK

Qasim A. Rafiq

Advanced Centre for Biochemical Engineering, Department of Biochemical Engineering, University College London, London, WC1E 6BT, United Kingdom

Aston Medical Research Institute, School of Life and Health Sciences, Aston University, Aston Triangle, Birmingham, B4 7ET

Centre for Biological Engineering, Loughborough University, Leicestershire, LE11 3TU, UK

Karen Coopman

Centre for Biological Engineering, Loughborough University, Leicestershire, LE11 3TU, UK

Bo Kara

FUJIFILM Diosynth Biotechnologies, Billingham, TS23 1LH, UK

*current address: GSK R&D, Gunnels Wood, Stevenage, Herts, SG1 2NY, UK

Christopher J. Hewitt,

Aston Medical Research Institute, School of Life and Health Sciences, Aston University, Aston Triangle, Birmingham, B4 7ET

Centre for Biological Engineering, Loughborough University, Leicestershire, LE11 3TU, UK

Author for correspondence:

Professor Christopher J. Hewitt, Aston Medical Research Institute, School of Life and Health Sciences, Aston University, Aston Triangle, Birmingham, B4 7ET. Email: c.j.hewitt@aston.ac.uk, Tel: +44 (0) 121 204 4949

Abstract

The impact of agitation rate and sparged aeration on BM-hMSC expansion in conventional stirred tank bioreactors was assessed. It was found that a decrease in impeller speed to below N_{JS} caused sampling difficulties, clumping and an increase to ~2 N_{JS} decreased the growth rate though an intermediate value of ~1.3 N_{JS} did not. Additionally, over this range of agitation intensities, cell quality remained unchanged post-harvest suggesting that poor growth performance at the highest speed was due to a failure of the cells to attach efficiently to microcarriers rather than damage to the cells due to fluid dynamic stress. Further it was shown that direct aeration of the culture medium both with and without Pluronic F68 *via* a sparger at N_{JS} was detrimental to BM-hMSC growth. Again, this reduction in growth seems to be associated with poor attachment rather than cell damage, which due to the mechanism of Pluronic™ F68 reducing the cell hydrophobicity and thus the affinity of the BM-hMSCs to attach to the microcarrier, leads to a poorer performance in the presence of the surfactant. Certain post-harvest quality characteristics are also detrimentally impacted compared to headspace aeration. This problem is discussed in terms of the need to facilitate future large-scale process development where headspace aeration at N_{JS} may not be sufficient to meet culture needs at higher cell densities.

Keywords

Process control, human mesenchymal stem cell, microcarrier expansion, harvest, agitation, aeration

1. Introduction

Bone marrow-derived human mesenchymal stem cells (BM-hMSCs) have generated much interest in the field of regenerative medicine and cell-base therapies, with the potential to treat and in some cases, cure human disease. This interest has been largely driven by their ability to proliferate under appropriate culture conditions and their capacity to secrete a range of trophic factors which regulate host immune response and initiate tissue repair [1]. Consequently, there have been approvals for BM-hMSC-based products and multiple trials involving the use of the cells are advancing through clinical development targeting indications such as cardiac repair, neurological disease and immune disorders [2]. Microcarriers have been used to culture adherent cells such as BM-hMSCs in suspension [3] allowing for process scale-up, where online monitoring and control systems can be used to deliver a consistent and cost-effective BM-hMSC therapy. Further to this, stirred-suspension bioreactors are currently employed in biopharmaceutical production and therefore their design and operation are well-understood [4], with the potential to meet the expected manufacturing demands of large-scale BM-hMSC therapies [5].

If the bioreactor is to work effectively, it is essential that the microcarriers are at least fully suspended in such a way that though they may regularly touch and move on the bottom, they do not remain stationary for any significant period of time, typically 5 s; that condition requires a certain minimum agitator speed to achieve it (usually given the symbol, N_{JS} (rev/s)) [6]. Under these conditions, the cells on the microcarrier are always surrounded by culture medium and are therefore able to take up nutrients (including O_2) from it and secrete growth-inhibiting metabolites into it. There is much emphasis in the literature on the sensitivity of cells grown on microcarriers to high fluid dynamic stresses generated by agitation such that the culture performance is poor whether dealing with animal cells for vaccine production or stem cells. There are a number of mechanisms that can give rise to mechanical stress on microcarriers and the cells on them; fluid motion relative to the microcarrier, impacts between microcarriers and the impeller or between microcarriers, and from bursting bubbles associated with the cells' oxygen demand. When growing cells, there are two ways in which culture may be compromised; one is growth and proliferation and the other, of critical importance for regenerative medicine and cell-based therapy applications, is cell or product quality. In the case of BM-hMSC, the cell forms the basis of the product. These issues in turn may arise for two reasons: the stress will detach the cells from the microcarriers and subsequently performance will be compromised or the stress will damage the cell while still on the microcarrier.

Meeting the oxygen demand of cells is often considered the process requirement needing the highest agitation intensity. At the cell density currently achievable and operating scale used at present when growing stem cells on microcarriers, in general, the most demanding agitation has been that required for microcarrier suspension and at this condition, the oxygen demand can be met by surface aeration. The same situation existed in the early days of free suspension mammalian cell culture, even though cell oxygen demand is an order of magnitude higher than BM-hMSCs [3]. But as cell densities increased to greater than 5 x 10^6 cells ml^{-1} and bioreactor scale increased, up to 25 m^3, aeration directly into the culture medium *via* the incorporation of a sparger had to be used [6]. This situation is likely to arise with stem cells in the future and this change may also create new challenges; for example, the addition of antifoam [7] into the medium, which has been previously shown to significantly reduce the mass transfer rate of the system [8]. It is also widely accepted that cell damage due to direct aeration in free suspension culture is primarily a result of cells attaching to bubbles and experiencing the huge energy release as they burst at the medium-air interface. Polymers such as Pluronic^{TM} F68 are widely used to decrease this cell damage and improve bioreactor performance [9, 10]. This improvement in performance by the addition of Pluronic^{TM} F68 is a result of its ability to reduce the hydrophobicity of the cell surface, preventing cell-bubble attachment and subsequent damage [11].

The aim of this study therefore, is to assess the impact of impeller agitation rate on BM-hMSC expansion in stirred bioreactors and the influence of direct aeration into the culture medium on the growth and characterization of BM-hMSC, to facilitate future large-scale development where headspace aeration at N_{JS} may not be sufficient.

2. Materials & Methods

2.1 Monolayer Culture

BM-hMSCs were isolated from bone-marrow aspirate purchased from Lonza (Walkersville, USA) obtained from a healthy donor with informed consent (lot: 071313B). The local Ethical Committee approved the use of the sample for research. Cells from passage 1 were cryopreserved at a density of 1-2 x 10^6 cells.ml^{-1} in a freeze medium containing 90% (v/v) FBS (Hyclone, Belgium) and 10% (v/v) dimethylsulphoxide (Sigma-Aldrich, UK). Cells were grown in T-flasks seeded at 5,000 cells.cm^{-2} at 37°C in humidified air containing 5% CO_2. For serum-free culture, the growth surface of T-flasks was coated with 0.4 µg.cm^{-2} PRIME-XV human fibronectin (FN) (Irvine Scientific, USA) and cultured in PRIME-XV MSC Expansion SFM (Irvine Scientific, USA) as per the manufacturer's instructions. On passage, the hMSCs were washed with phosphate buffered saline without Ca^+ or Mg^+ (PBS) and incubated for 4 min with TrypLE Express (Invitrogen, UK). Dissociation reagents were inactivated by the addition of appropriate growth medium and the cell suspension was centrifuged at 220g for 5 min. The supernatant was discarded and the remaining pellet was re-suspended in an appropriate volume of culture medium. BM-hMSCs underwent one adaptation passage in serum-free medium.

2.2 DASGIP DASbox bioreactor microcarrier culture

The glass surfaces of 250 ml DASGIP DASbox bioreactors (diam. T = 60 mm) (Eppendorf, Germany) were siliconized with Sigmacoat (Sigma-Aldrich, UK) according to manufacturer's instructions to prevent cell attachment to the surface of the bioreactor and impeller. The bioreactors were equipped with a 3-blade 30°-pitch, down pumping impeller (diameter, D = 30.25 mm), a temperature probe, a Hamilton dissolved oxygen (dO_2) probe, a Hamilton pH probe, an off-gas analyser and two sterile sample ports. Solid, non-porous Plastic P-102L microcarriers of 160-200 microns (Solohill, USA) were prepared to give 5000 cm^2/l per bioreactor following manufacturer's instructions. Microcarriers were coated with 0.1 µg.cm^{-2} PRIME-XV FN prior to hMSC inoculation at 6,000 cells. cm^{-2} and cultured in 100 ml of PRIME-XV MSC Expansion SFM with bioreactor control set-points of 37 °C and pH 7.4. A 50 % medium exchange was performed every two days as per manufacturer's instructions. Following inoculation, the culture was static for one hour (based on related work on optimizing attachment [12]) after which the culture was agitated at N_{JS} (found to be 115 rpm) or at whatever agitator speed was selected for that experiment both slightly below N_{JS} and well above it, with daily medium and cell-microcarrier samples of 1 ml taken for analysis. The DASbox system was set up, calibrated

and controlled using the DASGIP DASbox control unit (Eppendorf, Germany) and was operated with headspace aeration to achieve sufficient gas supply to give the desired oxygen concentration.

As pointed out above, the aim of this study was to assess the impact of impeller agitation intensity and bubbling aeration on BM-hMSC expansion in stirred bioreactors as part of an ongoing program to facilitate future large-scale development. The work on the impact of agitation was undertaken first and at that time, our earlier work conducted in an oxygen-controlled incubator for both monolayer [13] and spinner flask culture [14] indicated that with the same donor cells as cultured here, the performance with respect to growth kinetics was better at 100% dO_2.than at lower values when cultured over 3 passages. Thus, during the studies of agitation intensity, the dO_2 was controlled in the DASGIP DASbox bioreactor using the DASGIP DASbox control unit (Eppendorf, Germany) and was operated with headspace aeration to give 100% dO_2. However, subsequently during the present study in the DASGIP DASbox bioreactor [15], it was found that 25% dO_2 gave a better performance. So, whilst overall some literature studies have shown 100% dO_2 gives enhanced growth kinetics and others, lower dO_2 values [14], it was decided here to study the impact of air sparging at 25% dO_2. Thus, when investigating the impact of air sparging, the agitator speed was set at N_{JS} and the dO_2 was controlled to 25% when sparging at 0.1 VVM and also with headspace aeration.

Though both the topics relate to the cells' sensitivity to fluid dynamic stresses, they can also be viewed as somewhat separate issues as the potential mechanisms of damage are different.

2.3 DASGIP DASbox bioreactor harvest

BM-hMSCs were harvested using a method previously developed by us [16, 17]. Briefly, the DASbox control was switched off and the microcarriers allowed to settle. The spent culture medium was removed and the microcarriers were washed twice in 50 ml of Ca^{2+} and Mg^{2+} free PBS. The PBS was removed before adding 80 ml of TrypLE Express dissociation reagent for 10 minutes at an impeller speed of 375 rpm (ending with 5 seconds at 400 rpm). The dissociation reagent was then quenched with 70 ml of culture medium and a 2 ml sample placed in a single well of a 6 well plate for analysis under a light microscope to assess cell detachment. The remainder of the solution was filtered through a 60 μm Steriflip Filter Unit (Merck Millipore, Germany) to separate the microcarriers from the BM-hMSCs. The cell suspension was centrifuged, the supernatant aspirated

and the cell pellet re-suspended in culture medium. A cell count was then performed using a NucleoCounter NC-3000 to assess the overall hMSC growth and the culture harvest efficiency.

2.4 Analytical Techniques

Analysis of glucose and lactate concentrations in the spent medium was performed using a Cedex Bio-HT (Roche, Germany). Cell counting, mean cell diameter and viability (via acridine orange uptake and DAPI exclusion) was performed using a NucleoCounter NC-3000 automated mammalian cell counter (Chemometec, Denmark). The following parameters were obtained:

1. Specific Growth Rate

$$Specific\ growth\ rate, \mu = \frac{\ln\left({C_x(t)}/{C_x(0)}\right)}{\Delta t}$$

where μ is the net specific growth rate (h^{-1}), $C_x(t)$ and $C_x(0)$ are the cell numbers at the end and start of the exponential growth phase, respectively and t is time (h).

2. Population Doublings

$$Population\ Doublings, P_d = \frac{1}{\log\ (2)} \cdot \log\left(\frac{C_x(t)}{C_x(0)}\right)$$

where P_d is the number of population doublings, $C_x(t)$ and $C_x(0)$ are the cell numbers at the end and start of the exponential growth phase, respectively.

3. Specific Metabolite Consumption/Production Rate

$$Specific\ metabolite\ flux, q_{met} = \left(\frac{\mu}{C_x(0)}\right) \cdot \left(\frac{C_{met}(t) - C_{met}(0)}{e^{\mu t} - 1}\right)$$

where q_{met} is the net specific metabolite consumption or production rate, μ is the specific growth rate (h^{-1}), $C_x(0)$ is the cell number at the end of the exponential growth phase, $C_{met}(t)$ and $C_{met}(0)$ are the metabolite concentrations at the end and start of the exponential growth phase, respectively and t is time (h).

2.5 Colony-forming unit fibroblast (CFU-f) Efficiency

To assess the CFU-f efficiency, BM-hMSCs were seeded in a T-flask at 10 cells.cm^{-2} and cultured with a medium exchange every 3-5 days. Following 14 days culture, cells were washed with PBS and fixed in 4% formaldehyde (v/v) (Sigma, UK) for 30 minutes. Colonies were stained with 1% crystal violet (Sigma, UK) in 100% methanol (w/v) for 30 minutes. Stained colonies that were made up of more than 25 cells were recorded as CFUs.

2.6 hMSC Characterisation

Immunophenotype analysis was performed by multi-parameter flow cytometry before and after the hMSC expansion process using a previously developed protocol [18]]. Short Tandem Repeat analysis was completed by LGC Standards (UK) under their cell line authentication program. Morphology images were obtained using a light microscope (Nikon Eclipse TS-100, UK).

The hMSC differentiation was induced using PRIME-XV Differentiation SFM (Irvine Scientific, USA) as per manufacturer's instructions. After 21 days, the differentiation medium was removed, cells rinsed with PBS then fixed with 4% (v/v) PFA at room temperature. Adipocytes were stained with 1% (w/v) Oil Red O (Sigma-Aldrich, UK) in isopropanol at room temperature and rinsed with distilled water. Osteoblasts were incubated with 2.5% (v/v) silver nitrate (Sigma-Aldrich, UK) under ultraviolet light (30 minutes exposure), rinsed with distilled water and stained with fast violet solution (Sigma-Aldrich, UK) containing 4% (v/v) napthol AS-MX phosphate alkaline (Sigma-Aldrich, UK) for 45 minutes at room temperature in the dark. Chondrocytes were stained with 1% (w/v) Alcian blue (Sigma-Aldrich, UK) in 0.1 M hydrochloric acid (Sigma-Aldrich, UK). After 30 minutes incubation, cells were rinsed three times with 0.1 M HCl. After staining, differentiated cells were visualized under a light microscope (Nikon Eclipse TS-100, UK).

2.7 Statistical Analysis

Results were deemed to be significant if $p < 0.05$ using a two-tailed Students t-test.

3. Results & Discussion

3.1 Effect of agitation rate on BM-hMSC culture on microcarriers

3.1.1 Expansion

In order to support the successful expansion of BM-hMSCs on microcarriers in suspension bioreactors, it will be critically important to employ an agitation strategy that suspends the microcarriers without causing damage to the cells throughout scale-up and when higher cell densities are achieved. In order to quantify this requirement, the impact of different impeller speeds on the growth of BM-hMSCs on microcarriers has been assessed, whilst employing headspace aeration. In conjunction with this assessment, the critical turbulence parameters of the bioreactor system have been calculated to provide a strong theoretical basis for this comparison, which can be seen in Table 1.

Figure 1A shows the effect of the various impeller speeds on BM-hMSC growth from daily samples over six days, with the highest impeller speed of 225 rpm leading to the lowest BM-hMSC growth. This is confirmed by the post-harvest cell counts in Figure 1B, which shows that there is significantly lower ($p < 0.05$) BM-hMSC growth at the highest impeller speed. The minimum impeller speed to suspend the microcarriers (N_{JS}) was visually determined to be 115 rpm. Maintaining the microcarriers and cells in suspension is critical to ensure that effective mass transfer can take place [19] and to prevent attachment to the base of the bioreactor as well as severe cell-microcarrier clumping [14]. In addition, sampling during the run at 80 rpm was somewhat problematic as the microcarriers and cells were not entirely suspended and this explains why the daily cell concentration at 80 rpm (Figure 1A) was low compared with the post-harvest total cell number (Figure 1B). Therefore, though the post-harvest total cell number was the highest at this speed, the impeller speed in this microcarrier-based bioreactor system should still be at least 115 rpm.

Table 1 shows the characterization of the bioreactor system at different impeller speeds with a calculation of the Kolmogorov microscale of turbulence for each impeller speed [17]. Considering that the size of the microcarriers used in this study are in the range of 125-212 µm (mean size ~ 170 µm), Table 1 shows that the Kolmogorov microscale at each of the investigated impeller speeds is much less than the size of the microcarriers but much bigger than a BM-hMSC (~ 15 to 20 µm). Kolmogorov theory suggests that the eddies most likely to cause damage are those of the size of the suspended entity i.e. turbulent eddies which are the same size as the cell in free-suspension culture [20]. Croughan *et al* [20] investigated the impact of this microscale of

turbulence on animal cells grown on microcarriers, with cell damage becoming significant when the microscale was less than or equal to about two-thirds the size of the microcarriers. A similar result was found for the conditions used here in spinner flasks [17]. However, as found in studies in other agitated bioreactors of 15 ml and 5 l [17], based on the mean microcarrier size, that BM-hMSC growth kinetics were not affected at N_{JS} (115 rpm) even though the turbulent eddy size was < ~ 40% of the size of the microcarrier. Indeed, at 150 rpm (specific power input 0.06 W/kg) where the microscale was 1/3 of the size of the microcarrier, similar to that at N_{JS} in the 15 ml ambr [17], the growth rate was similar ($p > 0.05$) to that measured at N_{JS}, which is beneficial as the increased mean specific energy dissipation rate would enable higher oxygen demands to be met. At 225 rpm (mean specific energy dissipation rate 0.2 W/kg), the Kolmogorov scale is < 25% of that of the microcarriers and a severe reduction in performance was detected.

3.1.2 Metabolite flux

The relative flux of metabolites is an important parameter to measure and understand during the expansion process as it has the potential to form part of a process control system, based upon BM-hMSC characteristics. Figure 2A and B shows the lactate dehydrogenase (LDH) and total protein concentration at the various impeller speeds throughout the culture process, which do not increase as the impeller speed is changed. If cell damage was occurring during the culture process, the levels of LDH and total protein would increase [21]. The differences in BM-hMSC growth kinetics due to changes in impeller speed are therefore not attributed to cellular damage by membrane disruption in this instance. It has been demonstrated previously however, that increasing the shear stress in flow chambers during BM-hMSC culture leads to the inhibition of proliferation, in association with maintaining cells in the G0/G1 phase of the cell cycle [22]. Additionally, the reduction in growth kinetics at higher impeller speeds could be caused by an inhibition of BM-hMSC attachment and re-attachment to the microcarriers during the growth phase. Whatever the mechanism for the reduced growth rate of BM-hMSCs on microcarriers at increased impeller speeds, it is not caused by direct cell damage as is commonly assumed.

The net flux of each metabolite can be seen in Figure 3A and B, which shows an increase in ammonia production and yield of lactate from glucose at higher impeller speeds. The effect of impeller speed on the live metabolite concentrations during BM-hMSC expansion in controlled microcarrier culture can be seen in Supplementary Figure 1. The increased ammonia production at an impeller speed suggests altered amino acid utilisation, which may be related to the increased need for precursors (e.g., glutamine and asparagine)

supporting purine, and pyrimidine biosynthesis [23]. The yield of lactate from glucose for impeller speeds of 80, 115 and 150 rpm was around 2 $mol.mol^{-1}$ which indicates that the cells mainly metabolise glucose *via* the inefficient glycolytic pathway instead of oxidative phosphorylation [24]. The impeller speed of 225 rpm had a yield of lactate from glucose of 2.70 ± 0.73 $mol.mol^{-1}$ which is above the theoretical maximum yield of 2 $mol.mol^{-1}$ [25]. The high figure at 225 rpm suggests that an additional carbon source, most likely glutamine, is being metabolised to produce lactate and ammonia, resulting in higher lactate yields and an increase in the per cell ammonia flux [3] seen in Figure 3A. These findings are in line with previously published articles for both microcarrier and monolayer culture [26, 27].

3.1.3 Quality characteristics

In addition to the growth kinetics and metabolite flux, it is important to assess the post-harvest BM-hMSC characteristics to ensure that the process and harvest conditions have not had a detrimental impact on the quality of the cell [16]. The BM-hMSCs were harvested from the microcarrier surface and separated prior to characterization according to a previously published protocol for the DASGIP DASbox bioreactor platform [17], maintaining a post-harvest viability of >95% in all conditions. The specific outgrowth rate can be seen in Figure 4A which shows that the BM-hMSC post-harvest outgrowth rate was similar across all the impeller speeds investigated in the bioreactor. This similarity suggests that the impeller speed of 225 rpm has not triggered a senescent state in the BM-hMSCs or caused detriment to their outgrowth potential. This result is further evidence to support the hypothesis that the reduction of BM-hMSC growth kinetics on microcarriers at high impeller rates is due to inefficient cell-microcarrier attachment, rather than cell damage due to increasing fluid dynamic stresses. This finding also gives further support to the use of high agitation intensity as an aid to cell detachment during harvest [16, 17].

It can also be seen from Figure 4A that the post-harvest outgrowth kinetics of BM-hMSCs from the controlled DASbox bioreactor system at all impeller speeds were higher than either before expansion and post-harvest from the relatively-uncontrolled spinner flask process. This higher rate is an indication of the positive impact that control of the environment in the bioreactor is having on the BM-hMSC characteristics, which will be important for future bioprocess scale-up and development.

Associated with the increase in post-harvest outgrowth, the BM-hMSCs cultured in the DASbox bioreactor platform had a reduced mean cell diameter (Figure 4B) for all impeller speeds compared to pre-expansion and post-harvest from relatively-uncontrolled spinner flasks. As well as being associated with a decrease in BM-hMSC growth rate [28], an increase in cell size has been linked to aging of BM-hMSCs and loss in differentiation potential [29, 30] and therefore a reduction in BM-hMSC size through controlled microcarrier expansion will be beneficial to the manufacturing process. Colony forming potential has been highlighted as an important assay for the quality of BM-hMSC preparations [31] and is known to deteriorate during culture [32, 33]. Figure 4C shows the maintenance of colony forming potential from pre-expansion to post-harvest at all impeller speeds, which further demonstrates that the BM-hMSCs have not been damaged during the expansion and harvest process. Furthermore, BM-hMSCs have retained their immunophenotype and differentiation potential according to the ISCT minimum criteria (supplementary Figure 2).

3.2 Effect of sparged aeration on BM-hMSC culture on microcarriers

3.2.1 Expansion

Like agitation intensity, aeration strategies will play a key role in the successful development of microcarrier based bioreactor processes for BM-hMSC manufacture, particularly as the scale of operation and product cell density increases. Due to the fact that the specific oxygen demand and the cell densities achieved so far in BM-hMSC microcarrier culture are low, the oxygen demand of the cells in current benchtop bioreactors can be met by passing gas mixtures through the headspace. However, at the commercial scale, as the surface area to volume ratio is inversely proportional to scale, sparging will probably be required [4]. This issue is particularly important because in free suspension culture, bursting bubbles can be much more damaging than agitation and the addition of Pluronic F68 is required to prevent it [4].

To address this issue, BM-hMSCs have been cultured with sparged sub-surface aeration at 0.1 VVM, with and without Pluronic^{TM} F68 in the medium, and compared to headspace aeration, (all with dO_2 controlled at 25%). Figure 5A shows the growth rate over six days of bioreactor expansion, demonstrating that headspace aeration ($1.70 \pm 0.45 \times 10^5$ cell.ml^{-1} or $3.4 \pm 0.9 \times 10^4$ cell.cm^{-2}) supports significantly higher ($p < 0.05$) growth kinetics compared to sparged culture with ($0.52 \pm 0.15 \times 10^5$ cell.ml^{-1} or $1.04 \pm 0.3 \times 10^4$ cell.cm^{-2}) and without ($0.84 \pm 0.18 \times 10^5$ cell.ml^{-1} or $1.68 \pm 0.36 \times 10^4$ cell.cm^{-2}) Pluronic^{TM} F68. This study is the first indication that aeration directly into the culture medium *via* a sparger has a detrimental impact on the expansion of BM-hMSCs on

microcarriers. The cells ml^{-1} after 6 days when sparging in the presence of Pluronic^{TM} F68 is slightly higher than without it; and both are markedly lower than with headspace aeration. Interestingly, the addition of this surfactant has been shown to be effective in an alternative cell-microcarrier culture [34].

This results suggests that the detrimental impact of direct aeration on the microcarrier culture of BM-hMSCs is not simply due to cell-bubble attachment, with cell damage caused by subsequent bubble bursting at the gas-liquid interface as is the case with free suspension cell culture [11]. The key difference with the microcarrier culture of BM-hMSCs compared to free suspension cell culture is that the cells must adhere to the microcarrier surface prior to growth. The addition of Pluronic^{TM} F68 into the culture medium in this system is in fact having a detrimental impact on the growth of BM-hMSCs, which perhaps is not surprising given that the mechanism of Pluronic^{TM} F68 is to reduce the cell hydrophobicity, thus reducing the affinity of the BM-hMSCs to attach to the microcarrier or bubble surface. Further evidence of this hypothesis can be seen in Figure 5B, which shows the attachment rate of the BM-hMSCs to the microcarriers during the six days of culture. This figure shows that the attachment rate of the BM-hMSCs is reduced in sparged culture compared to headspace aeration, suggesting that introducing bubbles into the bioreactor system is disrupting the BM-hMSC attachment process. Additionally, the inclusion of Pluronic^{TM} F68 in the culture medium is further reducing the attachment rate of the BM-hMSCs to the microcarriers in suspension, in accordance with the mechanism described above. This reduced attachment rate of BM-hMSCs is likely to be contributing to the reduced growth rate seen under sparged conditions for BM-hMSCs cultured on microcarriers.

3.2.2 Metabolite flux

In addition to growth rate, the metabolite flux has been monitored throughout culture to assess the impact that direct aeration is having on the consumption and production of metabolites throughout microcarrier culture. Figure 6A, B and C show the per cell flux of glucose, lactate and ammonia respectively and Figure 6D, the yield of lactate from glucose throughout the six days of expansion for sparged and headspace aeration culture. These figures show that despite the reduced growth rate, the net flux of glucose, lactate and ammonia is similar for all conditions and again did not reach previously determined inhibitory levels at any point [35]**.** The per cell flux of each metabolite shows a similar level of net glucose consumption per cell in headspace and sparged aeration during culture. In contrast, the production of ammonia to above 3 $pmol.cell^{-1}.day^{-1}$ and lactate to above 20 $pmol.cell^{-1}.day^{-1}$ in sparged culture was significantly higher ($p < 0.05$) than from headspace aeration. The

increase in the per cell production of lactate and ammonia has previously been associated with a reduction in growth kinetics of BM-hMSCs throughout an expansion process [33]. As with the previous experiments, the LDH and total protein concentrations have been measured to assess whether any BM-hMSC stress or damage has been caused by sparged aeration. Supplementary Figures 3A and B show these concentrations throughout culture, which have not increased over the six-day period in any condition. This finding is further evidence to suggest that introducing sparged aeration into the culture is not causing cell damage by bubble bursting, as the level of LDH and total protein would be increasing throughout culture if cell damage was occurring, which is the likely reason why the addition of Pluronic^{TM} F68 into sparged culture is not improving the BM-hMSC growth rate on microcarriers. Considering that cell damage is not occurring during sparged aeration, this provides further evidence that the reduction in growth rate during direct aeration is caused by the reduction in attachment rate at the start of culture or increased detachment during culture.

3.2.3 Quality characterization

The post-harvest BM-hMSC number in Figure 7A further supports the previous findings, that a significantly higher ($p < 0.05$) number of BM-hMSCs were produced under headspace aeration, compared to sparged aeration in the controlled bioreactor process. Figure 7D shows that the post-harvest BM-hMSC mean diameter is increased for sparged culture, with a significant increase ($p < 0.05$) seen for sparged aeration with the addition of Pluronic^{TM} F68. This increase in post-harvest cell size is associated with a reduction in BM-hMSC attachment and subsequent growth rate with the addition of Pluronic^{TM} F68, as was seen previously for an impeller speed of 225 rpm. In addition to the increased post-harvest BM-hMSC diameter, the addition of Pluronic^{TM} F68 into the sparged culture lead to a reduction in BM-hMSC outgrowth kinetics (Figure 7C) as well as a significant reduction ($p < 0.05$) in the CFU potential of the BM-hMSCs (Figure 7B). This reduction raises concerns about the use of Pluronic^{TM} F68 in the culture of BM-hMSCs on microcarriers and its inclusion in cell-based therapy manufacturing processes should be carefully considered to ensure that it is not having a detrimental impact on the growth or quality of the cell product.

4. Conclusions

A range of impeller agitation speed have been used during the microcarrier expansion of BM-hMSCs from values below the minimum required to just suspend the microcarriers, N_{JS}, (the commonly recommended value for culture) to values ~ 2 N_{JS}. The lower value was to assess the impact of poor suspension; and higher values, the impact when the O_2 demand cannot be met at N_{JS} due to increasing cell density or scale. Though the

decrease to below N_{JS} gave the highest post-harvest total cell number, there were inconsistencies between pre and post because of sampling difficulties. In addition, poor suspension leads to increased clumping. At the other extreme at a speed of ~ 2 N_{JS}, the growth rate significantly decreased. However, at ~ 1.3 N_{JS}, the results were very similar to those at N_{JS}, indicating the potential for higher mass transfer rates from agitation. In addition, over this range of agitation intensity, there was not any detrimental impact on the BM-hMSC post-harvest re-growth characteristics.

Direct aeration of the culture medium both with and without Pluronic F68 in it *via* a sparger at N_{JS}, again relating to potential increasing mass transfer needs, has also been shown to be detrimental to BM-hMSC growth and certain post-harvest quality characteristics compared to headspace aeration. Direct aeration of the medium during bioreactor culture is not only likely to be required at the large-scale to supply oxygen to the cells but as importantly, to remove carbon dioxide. It is currently the preferred method of aeration and CO_2 stripping in large scale bioreactors for free suspension cell culture. Therefore, it will potentially be important during process scale-up; and to ensure that bioreactor parameters such as the specific energy dissipation rate and sparged aeration rates are not increased above levels which might affect the growth and quality characteristics of the BM-hMSC product. Thus, alternative methods of supplying sufficient levels of oxygen to microcarrier bioreactor systems culturing BM-hMSCs may have to be developed as well as establishing the level of pCO_2 that they can tolerate as these systems are scaled up to manufacture commercially-viable cell numbers.

Acknowledgments

This study has been funded by the Engineering and Physical Sciences Research Council (EPSRC) and FUJIFILM Diosynth Biotechnologies.

References

[1] Caplan AI, Dennis JE. Mesenchymal stem cells as trophic mediators. Journal of cellular biochemistry 2006;98:1076-84.
[2] Heathman TRJ, Nienow AW, McCall MJ, Coopman K, Kara B, Hewitt CJ. The translation of cell-based therapies: clinical landscape and manufacturing challenges. Regenerative medicine 2015;10:49-64.
[3] Rafiq QA, Brosnan KM, Coopman K, Nienow AW, Hewitt CJ. Culture of human mesenchymal stem cells on microcarriers in a 5 l stirred-tank bioreactor. Biotechnology letters 2013;35:1233-45.
[4] Nienow AW. Reactor engineering in large scale animal cell culture. Cytotechnology 2006;50:9-33.
[5] Simaria AS, Hassan S, Varadaraju H, Rowley J, Warren K, Vanek P, et al. Allogeneic cell therapy bioprocess economics and optimization: Single-use cell expansion technologies. Biotechnology and bioengineering 2014;111:69-83.
[6] Nienow AW. Aeration, Biotechnology. Kirk-Othmer Encyclopedia of Chemical Technology: John Wiley & Sons, Inc.; 2015.
[7] Mostafa SS, Gu X. Strategies for improved dCO2 removal in large-scale fed-batch cultures. Biotechnology progress 2003;19:45-51.
[8] Lavery M, Nienow AW. Oxygen transfer in animal cell culture medium. Biotechnology and bioengineering 1987;30:368-73.
[9] Kilburn DG, Webb FC. The cultivation of animal cells at controlled dissolved oxygen partial pressure. Reprinted from Biotechnology and Bioengineering Vol. X, Issue 6, Pages 801-814 (1968). Biotechnology and bioengineering 2000;67:657-70.
[10] Oh SKW, Nienow AW, Al-Rubeai M, Emery AN. The effects of agitation intensity with and without continuous sparging on the growth and antibody production of hybridoma cells. Journal of Biotechnology 1989;12:45-61.
[11] Meier SJ, Hatton TA, Wang DI. Cell death from bursting bubbles: role of cell attachment to rising bubbles in sparged reactors. Biotechnology and bioengineering 1999;62:468-78.
[12] Rafiq QA, Hanga MP, Heathman TRJ, Coopman K, Nienow AW, Williams DJ, et al. Process development of human multipotent stromal cell microcarrier culture using an automated high-throughput microbioreactor. Biotechnol Bioeng 2017;114:2253-66.
[13] Rafiq QA, Coopman K, Nienow AW, Hewitt CJ. A quantitative approach for understanding small-scale human mesenchymal stem cell culture - implications for large-scale bioprocess development. Biotechnology journal 2013;8:459-71.
[14] Nienow AW, Coopman K, Heathman TR, Rafiq QA, Hewitt CJ. Bioreactor Engineering Fundamentals for Stem Cell Manufacturing. In “Stem Cell Manufacturing”, (Eds. J.M.S. Cabral, C.L. de Silva, L. G. Chase and M. M. Diogo). Elsevier Science, Cambridge, USA 2017;Chapter 3:43-76.
[15] Heathman TR. Developing a process control stratgegy for the consistent and scalable manufacture of human mesenchymal stem cells. PhD thesis, Loughborogh University, UK 2015.
[16] Nienow AW, Rafiq QA, Coopman K, Hewitt CJ. A potentially scalable method for the harvesting of hMSCs from microcarriers. Biochemical Engineering Journal 2014;85:79-88.
[17] Nienow AW, Hewitt CJ, Heathman TRJ, Glyn VAM, Fonte GN, Hanga MP, et al. Agitation conditions for the culture and detachment of hMSCs from microcarriers in multiple bioreactor platforms. Biochemical Engineering Journal 2016;108:24-9.
[18] Chan AKC, Heathman TRJ, Coopman K, Hewitt CJ. Multiparameter flow cytometry for the characterisation of extracellular markers on human mesenchymal stem cells. Biotechnology letters 2014;36:731-41.
[19] Nienow AW. The suspension of solid particles. In: Harnby N, Edwards MF, Nienow AW (eds) Mixing in the process industries, 2nd edn.: Butterworth Heinemann, London; 1997. p. 364-93.
[20] Croughan MS, Hamel JF, Wang DIC. Hydrodynamic effects on animal cells grown in microcarrier cultures. Biotechnology and Bioengineering 1987;29:130-41.
[21] Lavrentieva A, Majore I, Kasper C, Hass R. Effects of hypoxic culture conditions on umbilical cord-derived human mesenchymal stem cells. Cell Commun Signal 2010;8:18.

[22] Luo W, Xiong W, Zhou J, Fang Z, Chen W, Fan Y, et al. Laminar shear stress delivers cell cycle arrest and anti-apoptosis to mesenchymal stem cells. Acta Biochimica et Biophysica Sinica 2011;43:210-6.
[23] Higuera GA, Schop D, Spitters TW, van Dijkhuizen-Radersma R, Bracke M, de Bruijn JD, et al. Patterns of amino acid metabolism by proliferating human mesenchymal stem cells. Tissue engineering Part A 2012;18:654-64.
[24] Higuera-Sierra G, Schop D, Janssen F, Dijkhuizen-Radersma R, Boxtel vAJB, Blitterswijk vCA. Quantifying in vitro growth and metabolism kinetics of human mesenchymal stem cells using a mathematical model. Tissue engineering Part A 2009;15:2653 - 63.
[25] Glacken MW. Catabolic Control of Mammalian Cell Culture. Nat Biotech 1988;6:1041-50.
[26] Heathman TR, Glyn VA, Picken A, Rafiq QA, Coopman K, Nienow AW. Expansion, harvest and cryopreservation of human mesenchymal stem cells in a serum-free microcarrier process. Biotechnol Bioeng 2015;112.
[27] Heathman TRJ, Stolzing A, Fabian C, Rafiq QA, Coopman K, Nienow AW, et al. Scalability and process transfer of mesenchymal stromal cell production from monolayer to microcarrier culture using human platelet lysate. Cytotherapy 2016;18:523-35.
[28] Heathman TRJ, Stolzing A, Fabian C, Rafiq QA, Coopman K, Nienow AW, et al. Serum-free process development: improving the yield and consistency of human mesenchymal stromal cell production. Cytotherapy 2015;17:1524-35.
[29] Wagner W, Ho AD, Zenke M. Different facets of aging in human mesenchymal stem cells. Tissue engineering Part B, Reviews 2010;16:445-53.
[30] Stolzing A, Scutt A. Age-related impairment of mesenchymal progenitor cell function. Aging cell 2006;5:213-24.
[31] Pochampally R. Colony forming unit assays for MSCs. Methods in molecular biology (Clifton, NJ) 2008;449:83-91.
[32] Schellenberg A, Stiehl T, Horn P, Joussen S, Pallua N, Ho AD, et al. Population dynamics of mesenchymal stromal cells during culture expansion. Cytotherapy 2012;14:401-11.
[33] Heathman TRJ, Rafiq QA, Chan AKC, Coopman K, Nienow AW, Kara B, et al. Characterization of human mesenchymal stem cells from multiple donors and the implications for large scale bioprocess development. Biochemical Engineering Journal 2016;108:14-23.
[34] Liu JY, Hafner J, Dragieva G, Burg G. Bioreactor microcarrier cell culture system (Bio-MCCS) for large-scale production of autologous melanocytes. Cell Transplant 2004;13:809-16.
[35] Schop D, Dijkhuizen-Radersma R, Borgart E, Janssen FW, Rozemuller H, Prins HJ. Expansion of human mesenchymal stromal cells on microcarriers: growth and metabolism. J Tissue Eng Regen Med 2010;4.

Figure Legends

Figure 1 – Effect of bioreactor impeller speed on BM-hMSC growth over six days of culture in the DASbox controlled bioreactor, showing (A) the increased cell concentration in the bioreactor over six days at all impeller speeds, (B) the significant fall ($p < 0.05$) in total post-harvest cell number at the highest impeller speed. Control set-points are 100% dissolved oxygen and pH 7.4 with headspace aeration. Data shows mean ± SD, n = 3.

Figure 2 – Effect of impeller speed on A) the production of lactate dehydrogenase (LDH) and B) total protein concentration during microcarrier culture of BM-hMSCs in a controlled bioreactor. Showing no significant increase in LDH concentration or total protein at various impeller speeds, demonstrating low levels of cell damage during culture. Data shows mean ± SD, n = 3.

Figure 3 – Effect of bioreactor impeller speed on BM-hMSC metabolite flux over six days of culture in the DASbox controlled bioreactor, showing (A) per cell flux of ammonia and (B) yield of lactate from glucose. Control set-points are 100% dissolved oxygen and pH 7.4 with headspace aeration. Data shows mean ± SD, n = 3.

Figure 4 – Post-harvest characteristics of BM-hMSCs from controlled microcarrier culture compared to spinner flasks [14]. Showing (A) increased outgrowth kinetics, (B) reduced mean cell diameter and (C) maintained CFU efficiency all impeller speeds. Data shows mean ± SD, n = 3.

Figure 5 – Effect of sparging (VVM = 0.1) with and without Pluronic^{TM} F68 on BM-hMSC growth over six days of controlled microcarrier culture compared to headspace aeration. Showing (A) significantly increased growth rate with headspace aeration ($p < 0.05$), and (B) reduced BM-hMSC attachment in sparged culture, particularly with the addition of Pluronic^{TM} F68. Control set-points are 115rpm impeller speed, 25% DO concentration and pH 7.4. Data shows mean ± SD, n = 3.

Figure 6 – Effect of sparging (VVM = 0.1) with and without Pluronic^{TM} F68 compared to headspace aeration on BM-hMSC metabolite flux over six days of controlled microcarrier culture . Showing (A) similar glucose consumption rate, (B) increased lactate production, (C) significantly increased ammonia production rate ($p < 0.05$) and (D) similar yield of lactate from glucose in sparged culture. Control set-points are 115rpm impeller speed, 25% dO_2 concentration and pH 7.4. Data shows mean ± SD, n = 3.

Figure 7 – Effect of sparging (VVM = 0.1) with and without Pluronic^{TM} F68 on BM-hMSC attachment and post-harvest characteristics after six days of controlled microcarrier culture compared to headspace aeration. Showing (A) significantly reduced harvest cell number ($p < 0.05$), (B) decreased CFU efficiency, (C) similar specific outgrowth rate and (D) significantly increased mean cell diameter in sparged culture ($p < 0.05$). Control set-points are 115rpm impeller speed, 25% dO_2 concentration and pH 7.4. Data shows mean ± SD, n = 3.

Table 1 –Fluid dynamic characterisation of the DASGIP DASbox bioreactor platform at the various impeller speeds used in this study (impeller diameter of 0.03 m and a bioreactor diameter of 0.063 m). (Based on the procedure set out in Nienow et al. 2016 [17]).

Supplementary Figures

Supplementary Figure 1 – Effect of impeller speed on the live metabolite concentrations during BM-hMSC expansion in controlled microcarrier culture at 100% dO_2 with headspace aeration. Showing (A) glucose, (B) lactate and (C) ammonia concentrations at various impeller speeds. Data shows mean ± SD, n = 3.

Supplementary Figure 3 – Effect of aeration method on the metabolite flux of BM-hMSCs in controlled microcarrier culture. Showing no significant increase in (A) LDH concentration or (B) total protein with various

aeration methods, demonstrating low levels of cell damage during culture. Control set-points are 115rpm impeller speed, 25% dO_2 concentration and pH 7.4. Data shows mean ± SD, n = 3.

Supplementary Figure 2 - Verification of post-harvest immunophenotype and differential potential of BM-hMSCs used during this study in accordance with the ISCT minimum criteria.

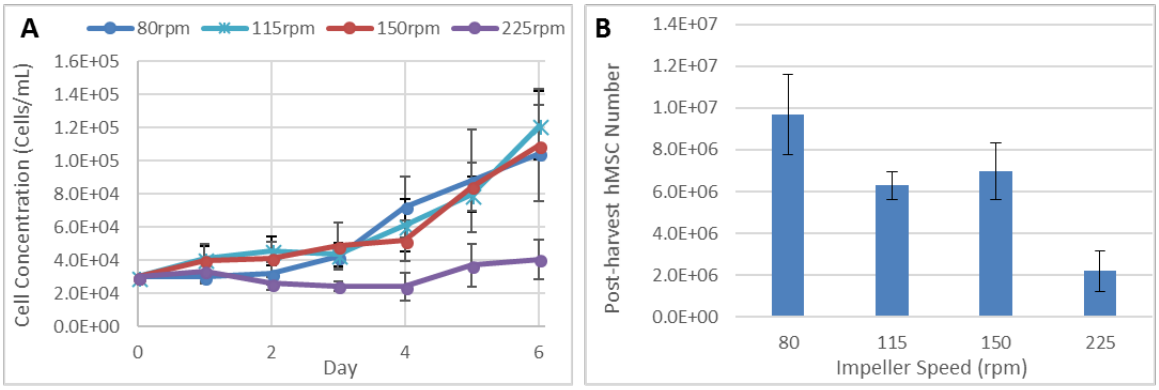


Figure 1 – Effect of bioreactor impeller speed on BM-hMSC growth over six days of culture in the DASbox controlled bioreactor, showing (A) the increased cell concentration in the bioreactor over six days at all impeller speeds, (B) the significant fall ($p < 0.05$) in total post-harvest cell number at the highest impeller speed. Control set-points are 100% dissolved oxygen and pH 7.4 with headspace aeration. Data shows mean ± SD, n = 3.

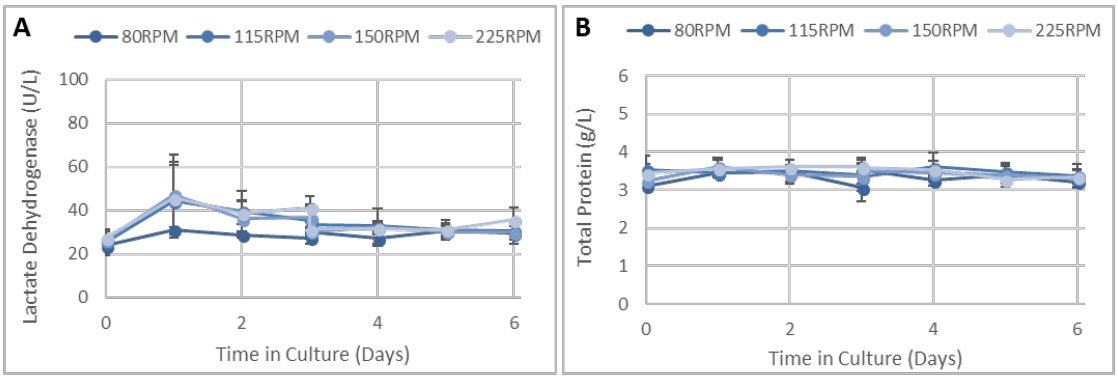


Figure 2 – Effect of impeller speed on A) the production of lactate dehydrogenase (LDH) and B) total protein concentration during microcarrier culture of BM-hMSCs in a controlled bioreactor. Showing no significant increase in LDH concentration or total protein at various impeller speeds, demonstrating low levels of cell damage during culture. Data shows mean ± SD, n = 3.

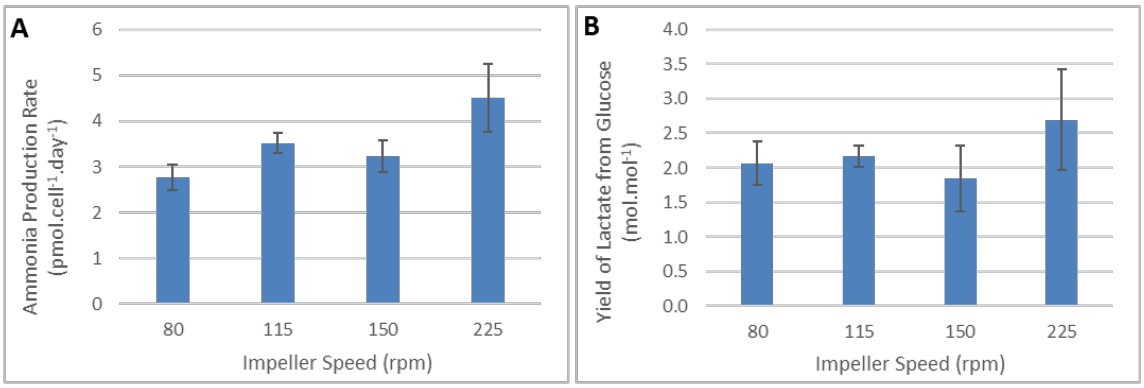


Figure 3 – Effect of bioreactor impeller speed on BM-hMSC metabolite flux over six days of culture in the DASbox controlled bioreactor, showing (A) per cell flux of ammonia and (B) yield of lactate from glucose. Control set-points are 100% dissolved oxygen and pH 7.4 with headspace aeration. Data shows mean ± SD, n = 3.

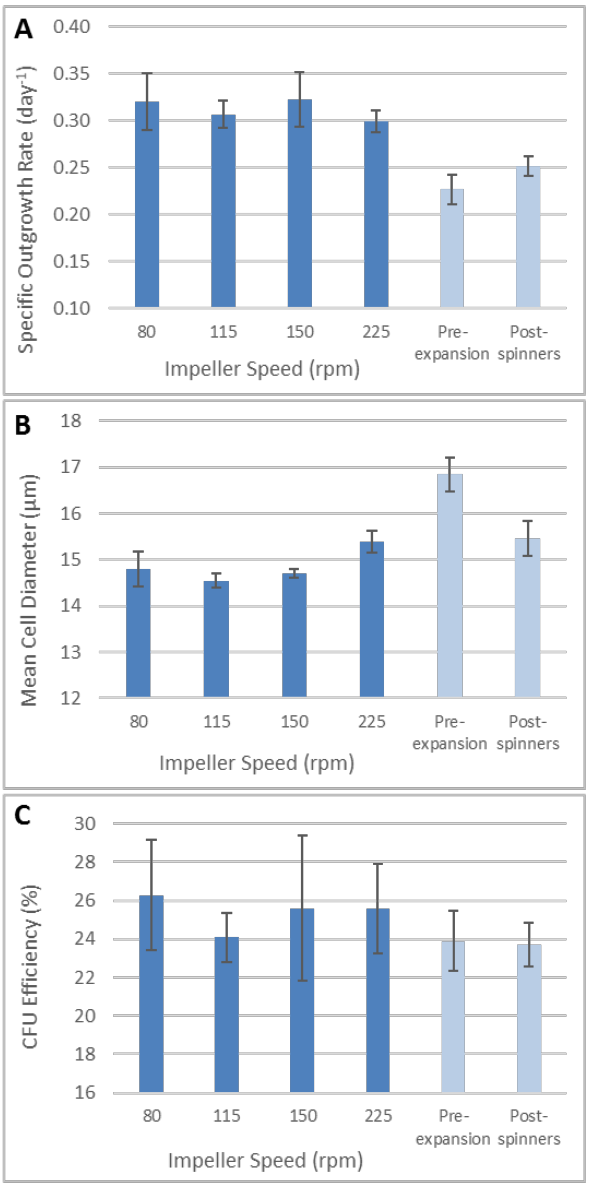


Figure 4 – Post-harvest characteristics of BM-hMSCs from controlled microcarrier culture compared to spinner flasks [14]. Showing (A) increased outgrowth kinetics, (B) reduced mean cell diameter and (C) maintained CFU efficiency at all impeller speeds. Data shows mean ± SD, n = 3.

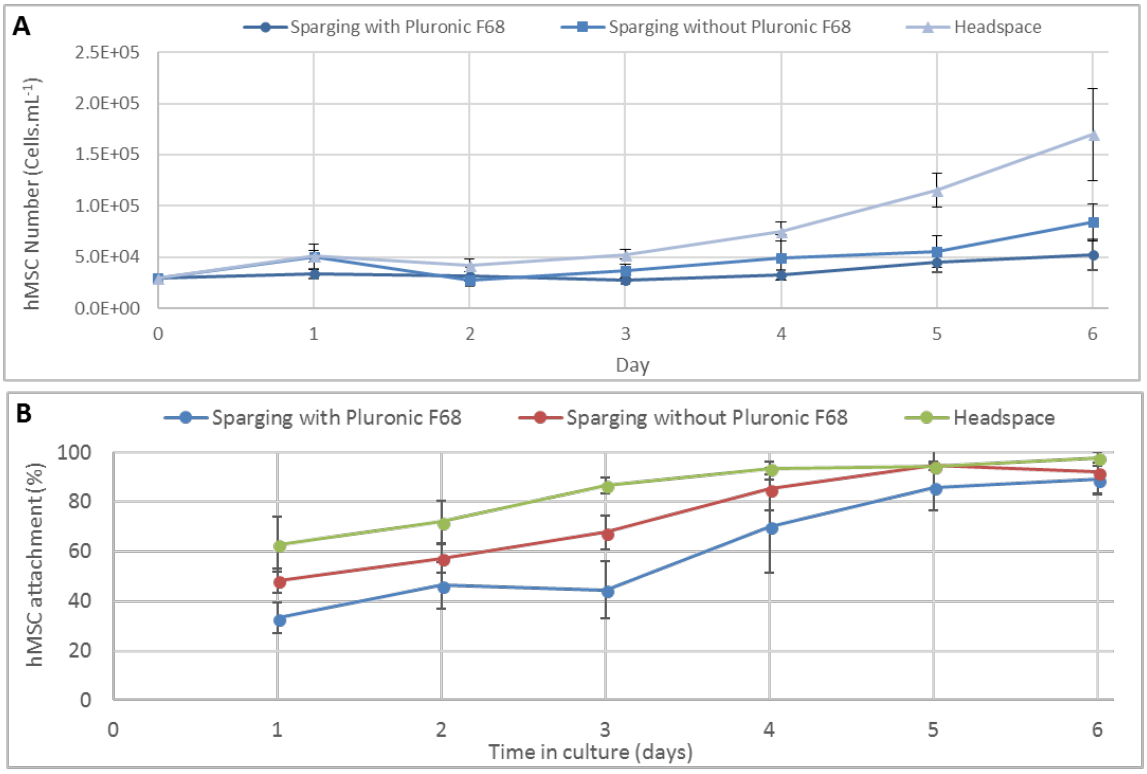


Figure 5 – Effect of sparging (VVM = 0.1) with and without Pluronic™ F68 on BM-hMSC growth over six days of controlled microcarrier culture compared to headspace aeration. Showing (A) significantly increased growth rate with headspace aeration ($p < 0.05$), and (B) reduced BM-hMSC attachment in sparged culture, particularly with the addition of Pluronic™ F68.. Control set-points are 115 rpm impeller speed, 25% dO_2 concentration and pH 7.4. Data shows mean ± SD, n = 3.

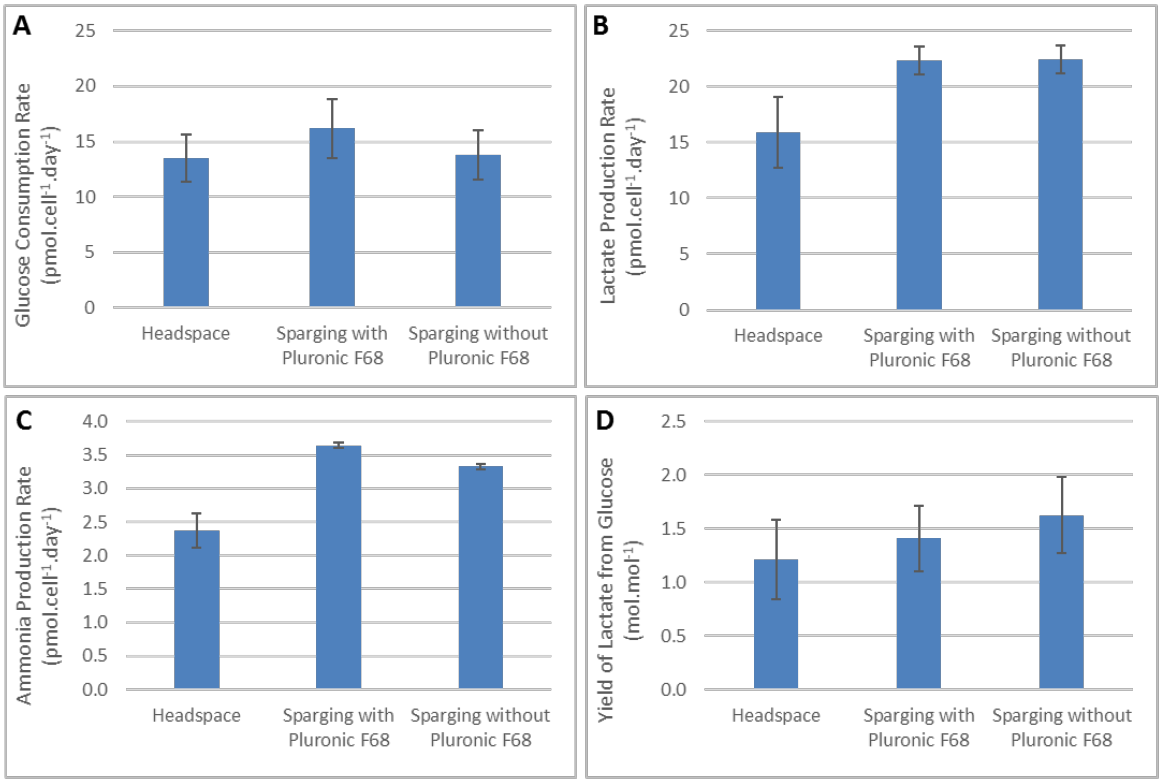


Figure 6 – Effect of sparging (VVM = 0.1) with and without Pluronic™ F68 compared to headspace aeration on BM-hMSC metabolite flux over six days of controlled microcarrier culture . Showing (A) similar glucose consumption rate, (B) increased lactate production, (C) significantly increased ammonia production rate ($p < 0.05$) and (D) similar yield of lactate from glucose in sparged culture Control set-points are 115 rpm impeller speed, 25% dO_2 concentration and pH 7.4. Data shows mean ± SD, n = 3.

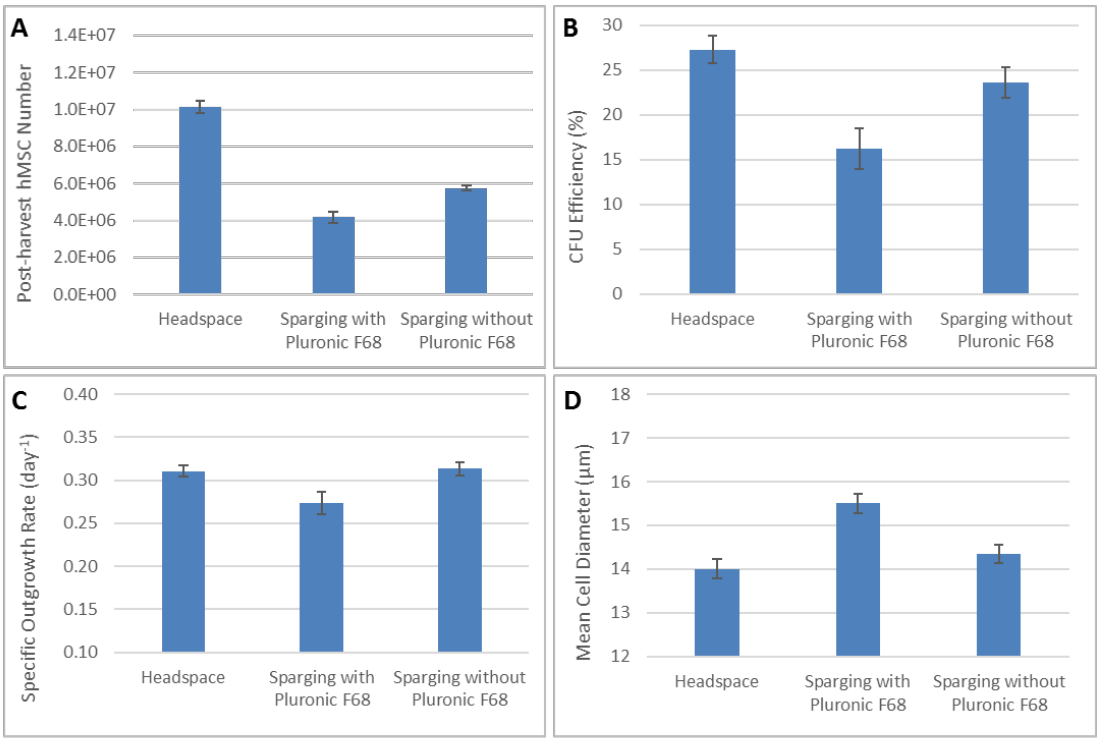
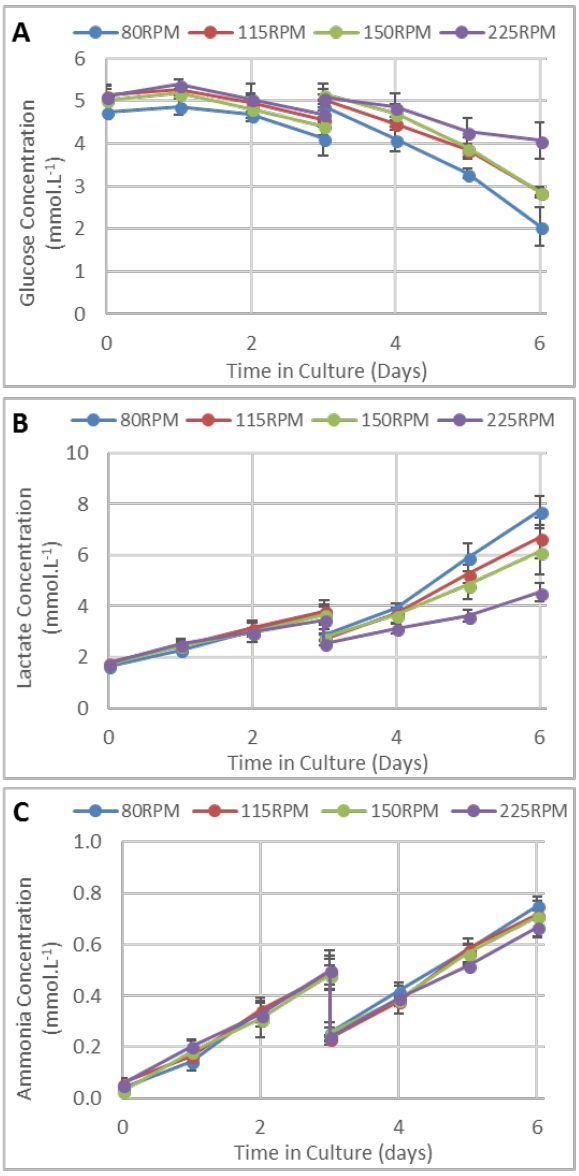


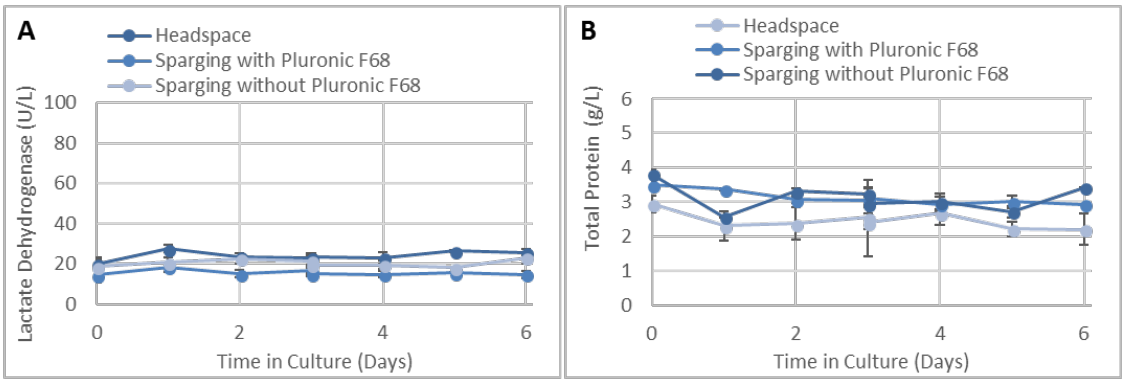
Figure 7 – Effect of sparging (VVM = 0.1) with and without Pluronic™ F68 on BM-hMSC attachment and post-harvest characteristics after six days of controlled microcarrier culture compared to headspace aeration. Showing (A) significantly reduced harvest cell number ($p < 0.05$), (B) decreased CFU efficiency, (C) similar specific outgrowth rate and (D) significantly increased mean cell diameter in sparged culture ($p < 0.05$). Control set-points are 115rpm impeller speed, 25% dO_2 concentration and pH 7.4. Data shows mean ± SD, n = 3.

Impeller rate (rpm)	Culture volume (ml)	Power number[1]	Max dissipation rate/average dissipation rate[1]	Reynolds number	Impeller speed (s^{-1})	Max specific energy dissipation rate (W/kg)	Kolmogorov scale of turbulence (µm)
80	100	1.5	18	1440	1.33	0.016	90
115	100	1.5	18	2070	1.92	0.046	68
150	100	1.5	18	2700	2.50	0.103	56
225	100	1.5	18	4050	3.75	0.346	41

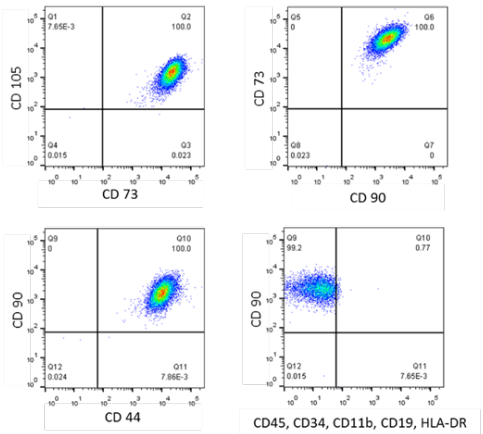
Table 1 – Fluid dynamic characterisation of the DASGIP DASbox bioreactor platform at the various impeller speeds used in this study (impeller diameter of 0.03 m and a bioreactor diameter of 0.063 m). (Based on the procedure set out in Nienow et al. 2016 [17]).

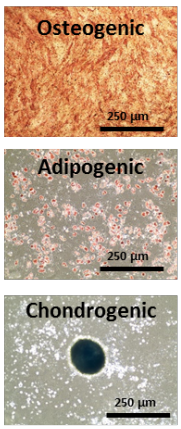


Supplementary figure 1 – Effect of impeller speed on the live metabolite concentrations during BM-hMSC expansion in controlled microcarrier culture at 100% dO_2 with headspace aeration. Showing (A) glucose, (B) lactate and (C) ammonia concentrations at various impeller speeds. Data shows mean ± SD, n = 3.



Supplementary figure 3 – Effect of aeration method on the metabolite flux of BM-hMSCs in controlled microcarrier culture. Showing no significant increase in (A) LDH concentration or (B) total protein with various aeration methods, demonstrating low levels of cell damage during culture. Control set-points are 115rpm impeller speed, 25% dO_2 concentration and pH 7.4. Data shows mean ± SD, n = 3.





Impeller speed (rpm)	% co-expression of immunophenotye markers
80	96.50 ± 0.14
150	96.80 ± 0.28
225	95.80 ± 0.14

Supplementary figure 2 - Verification of post-harvest immunophenotype and differential potential of BM-hMSCs used during this study in accordance with the ISCT minimum criteria.